An Efficient Mobility Management Scheme for 5G Network Architectures

Ioannis Kosmopoulos[1], Emmanouil Skondras[1], Angelos Michalas[2], Dimitrios D. Vergados[1]
[1]Department of Informatics, University of Piraeus, Piraeus, Greece, Email: {kosmopoulos, skondras, vergados}@unipi.gr
[2]Department of Informatics, University of Western Macedonia,
Kastoria, Greece, Email: amichalas@uowm.gr

***Abstract*—Fifth generation (5G) networks use heterogeneous network access technologies to support Mobile Nodes (MNs) with multiple services with different Quality of Service (QoS) constraints. In a 5G architecture, an MN can use Massive Multiple Input Multipole Output (MMIMO) antennas to obtain access to increased telecommunication resources. In these environments the need to support service continuity of MNs is a key issue. Therefore, the design of efficient mobility management schemes for 5G infrastructures is needed. In this paper, a novel mobility management scheme for 5G systems is proposed. Whenever the perceived Quality of Service (QoS) becomes less than a predefined threshold, Vertical Handover (VHO) is initiated. Subsequently, network selection is performed, considering the energy level of the MN. Finally, a MIH-enhanced FPMIPv6 handover approach is performed to achieve service continuity of the MNs. The proposed scheme is applied to a 5G architecture which includes LTE-A Pro FD-MIMO Macrocell, LTE-A and 802.16 WiMAX Femtocells, as well as 802.11p WAVE Road Side Units (RSUs). Performance evaluation shows that the suggested method ensures the Always Best Connection (ABC) principle. Also, the time that the MN remains functional is increased since it selects networks with decreased energy requirements when its energy level becomes low. Furthermore, the signaling cost of the proposed scheme is lower than the one observed from the use of other mobility management protocols.**

***Index Terms*—Mobility Management, 5G, Massive MIMO, LTE-A Pro, WAVE, WiMAX**

I. Introduction

The 5th generation wireless networks support revolutionary services for modern Mobile Nodes (MNs). Heterogeneous network access technologies, including the 3GPP Long Term Evolution Advanced (LTE-A), the IEEE 802.16 WiMAX and the IEEE 802.11p Wireless Access for Vehicular Environment (WAVE) usually co-exist. Also, Massive Multiple Input Multiple Output (MMIMO) antennas can be used to increase the bandwidth that each MN perceives. Additionally, Software Defined Networking (SDN) [1] is an emerging technology that centralizes the network intelligence enhancing the flexibility of resource manipulation. More specifically, the network control functions are decoupled from the data forwarding procedures while the network architecture becomes easily programmable. Thus, resource optimization is achieved by dynamically adjusting the traffic forwarding to meet the changing needs that exist in the modern wireless communication environment. In such a context, connectivity to the most suitable network is required for the MNs travelling across networks. Several factors need to be considered in such complex access environments. In particular, seamless handover schemes should be applied exhibiting low latency and maintaining the required level of QoS. Additionally, since the use of MMIMO increases the energy consumption of MNs which usually embed limited energy resources, optimized manipulation of MNs mobility management is required.

In this paper, an effective energy aware vertical handover scheme is proposed. The proposed approach complements the functionalities of FPMIPv6 with the MIH standard, to support the handover operation while it fulfils the MN's requirements for its transition to the best possible new access network. The described methodology is evaluated through simulations in a heterogeneous wireless network architecture consisting of LTE-A, 802.16 WiMAX and 802.11p WAVE networks.

The remainder of the paper is as follows: Section II describes the related work, while Section III presents the proposed scheme. Subsequently, Section IV presents the simulation setup and the evaluation results. Finally, section V concludes the discussed work.

II. Related Work

Several protocols performing mobility management in heterogeneous network architectures have been proposed from the industrial and research communities. These standards include the Mobile IPv6 (MIPv6) [2], [3], the Fast Handover Mobile IPv6 (FMIPv6) [4], the Proxy Mobile IPv6 (PMIPv6) [5] and the Fast Handovers for Proxy Mobile IPv6 (FPMIPv6) [6].

In [2], the use of the MIPv6 in IEEE 802.16e WiMAX network architectures is proposed. Specifically, using the MIPv6, mobile users prevent data losses by maintaining their IP address during their movement inside the area of the multiple WiMAX access networks. Experimental results showed that the proposed scheme eliminates the data losses observed during the users' mobility.

In [4], the authors conduct a comprehensive analysis inspecting the MIPv6 and FMIPv6 operations in Low Earth Orbit (LEO) satellite networks. Performance evaluation results have shown that the FMIPv6 outperforms the MIPv6

978-1-7281-6445-8/20/$31.00

in handover latency, forwarding cost and packet loss. Also, experimental results confirm the significance of utilizing the handover success rate and tunneling mechanisms in FPMIPv6 solutions.

Authors in [5], propose a software defined network (SDN) which extends the PMIPv6 implementation by constructing an OpenFlow based PMIPv6 (OF-PMIPv6) handover mechanism. The architecture separates the control and the data planes. Specifically a centralized control entity performs mobility control and the data flows remain between the Mobile Access Gateway (MAG) and the Local Mobility Anchor (LMA). Based on the OF-PMIPv6 architecture, reactive and proactive schemes achieve improvement in packet loss and handover latency.

In [6], the authors introduce a security environment to the HO process. The FPMIPv6 can guarantee a seamless handover, however the privacy and security issues are not accommodated. Accordingly, they propose the MIH-SPFP scheme for Fast Proxy Mobile IPv6-IoT networks which enhances security for intra- and inter- MAG handovers by providing a safeguarded and low latency channel.

In [7] a MIH enhanced FPMIPv6 scheme is presented considering the functionalities of the Evolved Packet Core (EPC) [8]. Specifically, the authors propose a VHO scheme that applies the IEEE 802.11 MIH protocol to the EPC architecture to facilitate a seamless handover. Furthermore, direct routing of downlink and uplink packets is performed. Also, the transient flag is introduced to avoid ping-pong effects and false handovers by retaining the initial and transient binding for packet exchange. Experimental results showed the effectiveness of the proposed scheme over the FPMIPv6 in handover latency, overall signaling cost and packet loss parameters.

In [9] the RSS Threshold Based Dynamic Heuristic (RTBDH), the QoS Based Heuristic (QBH), the SINR Based Heuristic (SBH) and the Weight Function Based Heuristic (WFBH) VHO decision algorithms are discussed. Specifically, the RTBDH algorithm uses dynamic RSS thresholds to reduce the number of incorrect or unnecessary handovers. Similarly, the SBH algorithm uses a SINR based method to perform HO. By utilizing the concept of QoS, the QBH algorithm considers the residual bandwidth and user service requirements for the HO decisions. Also, the WFBH algorithm uses a cost function to evaluate the QoS that each available network offers. In case that the QoS of the current network is lower that the other available networks, the network with the highest QoS is selected as the HO target.

In addition to the aforementioned works, Multi Attribute Decision Making (MADM) methods can be used to select the best alternative among candidate networks to handover. Widely used methods include the Analytic Hierarchy Process (AHP) [10], the Analytic network process (ANP) [11], the Technique for Order Preference by Similarity to Ideal Solution (TOPSIS) [12], the Trapezoidal Fuzzy TOPSIS (TFT) [13], the Dynamic TOPSIS (DTOPSIS) [14], the Simple Additive Weighting (SAW) [10] [15], the Fuzzy SAW (FSAW) [16], the Multiplicative Exponential Weighting (MEW) [10] and the Fuzzy MEW (FMEW) [17].

III. The Proposed Algorithm

In general, the VHO process is divided into three phases, namely the VHO initiation, the network selection and the VHO execution. As the MN moves inside a heterogeneous network environment, the VHO initiation evaluates the necessity to perform a handover. Subsequently, the network selection phase ranks the available network alternatives and selects the one with the highest ranking. Finally, during the VHO execution the appropriate signaling is exchanged between the MN and the network infrastructure, in order for the MN to be connected to the selected network. Figure 1 presents the proposed methodology, while the following subsections describe the VHO initiation, the network selection and the VHO execution processes for the predictive VHO scenario of FPMIP. As it is already mentioned our scheme considers the QoS perceived the MNs as well as the energy level of MNs during the selection process. Also, at the execution phase an improved FPMIP approach is proposed to reduce signaling costs, packet delays and losses during handover, while MIH functionality is included to facilitate the mobility operation.

A. VHO Initiation

During the VHO initiation, the QoS level $C_{j,s,i}$ that the j^{th} MN perceives for the s^{th} service from its current PoA i is considered. Specifically, $C_{j,s,i}$ depends on the available bandwidth $B_{j,i}$ and on the observed Signal to Interference plus Noise Ratio ($SINR_{j,i}$). Based on to Shannon's theorem, the $C_{j,s,i}$ is estimated using the following formula:

$$C_{j,s,i} = B_{j,i} \cdot log_2(1 + SINR_{j,i} \cdot W_s) \quad (1)$$

where W_s represents the relative importance of each service. When the observed $C_{j,s,i}$ drops below a predefined threshold the MN sends a $1.MIH\_Data\_Rate\_Going\_down$ message to the serving MAG. Following the serving MAG starts buffering downlink packets received from the network and the network selection follows.

B. Network Selection

During the network selection, initially the current MAG requests the MIIS to provide information about the neighboring networks through a $2.MIH\_GET\_Information\_request$ message, which determines the required minimum data rate and the remaining energy of the MN. The MIIS constructs a list with the candidate PoAs. The list includes the PoAs that provide a data rate greater than a specified threshold, while at the same time comply with the energy requirements of MN. The MIIS controller ranks the candidate PoAs using the formula (1) and sorts them in descending order according to their ranks. PoAs with high energy demands (e.g. FD-MIMO PoAs which use multiple antennas) are not included as candidate networks for MNs with low energy levels, since this situation will decrease significantly their energy levels and therefore their functionality. Subsequently, the current

MAG receives the sorted list of the candidate PoAs from the MIIS through a $3.MIH\_GET\_Information\_response$ message. The current MAG checks the availability of the resources of each candidate PoA by exchanging $4.MIH\_N2N\_HO\_Resource\_request$ and $5.MIH\_N2N\_HO\_Resource\_response$ messages with them, until a PoA with the required resources for performing a handover to be found. Since the messages 4 and 5 are exchanged using the aforementioned sorted list of candidate PoAs, decreased signalling cost is observed.

C. VHO execution

During the VHO execution, the current MAG initially reserves the necessary resources at the new MAG for the upcoming handover by exchanging the $6.MIH\_N2N\_HO\_Commit\_request$ and $7.MIH\_N2N\_HO\_Commit\_response$ messages with it. Subsequently, the current MAG informs the MN about the resource allocation through a $8.MIH\_Net\_HO\_Commit\_request$ message, while the MN acknowledges the reception of the information using a $9.MIH\_Net\_HO\_Commit\_responce$ message. Then, the current MAG provides the new MAG with the related information including the MN Identifier (MN-ID), the MN Logical Link Identifier (MN-LLID) and the LMA Address (LMAA) serving the MN by sending the $10.Handover\_Initiate$ message. The new MAG replies back with the $11.Handover\_Ack$ message and a bi-directional tunnel is established between the two entities. Afterwards, a copy of the buffered packets form the current MAG are transmitted through the IP-tunnel to the new MAG for delivery to the MN when the later connects to the new PoA. Subsequently, the candidate MAG sends the $12.PBU$ message to the LMA to create a transient record in the binding cache. It should be noted that the PBU message has set the B (Buffering), the T (Transient) and the P (Proxy) flags to 1. As soon as the LMA receives the PBU message, it starts buffering downlink packets received from the network.

Once the temporal binding is created at the BCE of the LMA, the $13.PBA$ message is sent to the new MAG and a temporal binding is established between the two entities. As a result, downlink packets are forwarded from the LMA to the new MAG where they are buffered for delivery to the MN when it connects at the new PoA. In this context, the bi-directional channel between the current MAG and the LMA remains active until the transient binding becomes permanent. Therefore, the transient binding introduces a smooth way for performing handover by gradually changing the serving MAG to avoid packet losses and false handovers. When the MN attaches to the new PoA its MIHF entity sends a $14.MIH\_Link\_up$ message to the candidate PoA to inform it that the communication channel is active and ready to receive packets. Also, the MN sends a $15.UNA$ to the candidate MAG, to inform it that the link and the IP layer have been established. The new MAG updates and finalizes the binding using the $16.PBU$ and $17.PBA$ messages. Also, the resources of the current MAG are released using the $18.MIH\_N2N\_Complete\_request$ and $19.MIH\_N2N\_Complete\_response$ messages. Finally, the bi-directional tunnel established between the two MAGs is released, while at the same time packets reach the MN through the new PoA/MAG, which hereinafter can be referred to as the current PoA/MAG.

IV. Simulation Setup and Results

In our experiments, the 5G topology presented in figure 2 is simulated. The network topology is being built using the Network Simulator 3 (NS3) simulator [18]. It includes a Fog and a Cloud infrastructure. The Fog infrastructure includes an LTE-A Pro FD-MIMO Macrocell, an LTE-A Femtocell, a WiMAX Femtocell and two WAVE RSUs, along with the corresponding Medium Access Gateways (MAGs) installed on them. Also, each MAG includes a MIH-enhanced PMIPv6 entity. Additionally, the Fog infrastructure includes an SDN controller which contains the MIIS and the LMA/AAA entities. The SDN controller also includes a Fog Manager which manipulates the allocation of the Fog resources. The Cloud infrastructure includes a set of Virtual Machines (VMs) providing Video, VoIP and IoT services, as well as a Software Defined Cloud (SDC) controller. The SDC controller includes a Cloud Manager which manipulates the allocation of the Cloud resources.

We consider the case where 10 Mobile Nodes (MN) are moving inside the network environment and need to be connected to a PoA which satisfies the requirements of their services. Table I presents the current PoA of each MN.

TABLE I: The current PoA of each MN.

Mobile Node	Current PoA
MN0	WAVE RSU 2
MN1	LTE-A Femtocell
MN2	LTE-A Pro FD-MIMO Macrocell
MN3	WiMAX Femtocell
MN4	WAVE RSU 1
MN5	WAVE RSU 1
MN6	WAVE RSU 2
MN7	WiMAX Femtocell
MN8	WAVE RSU 2
MN9	WAVE RSU 2

A. Evaluation of the VHO initiation & network selection

The VHO initiation & network selection functionalities of the proposed scheme are evaluated in comparison with the WFBH decision algorithm [9]. Regarding the simulation parameters, the LTE-A Pro FD-MIMO Macrocell offers $B_i = 100MHz$, the WAVE RSU offers $B_i = 10MHz$, while the LTE and the WiMAX Femtocells offer $B_i = 20MHz$ each. Additionally, in our experiments, for the calculation of the $C_{j,Video,i}$, $C_{j,VoIP,i}$ and $C_{j,IoT,i}$ values the relative importance W_s of each service has been set considering the service constraints as they are explained in the LTE QoS class specifications [19], [20]. Specifically, $W_{Video} = 0.5$, $W_{VoIP} = 0.35$ and $W_{IoT} = 0.15$. The threshold values are calculated by considering $SINR = 14db$ as proposed in [21]

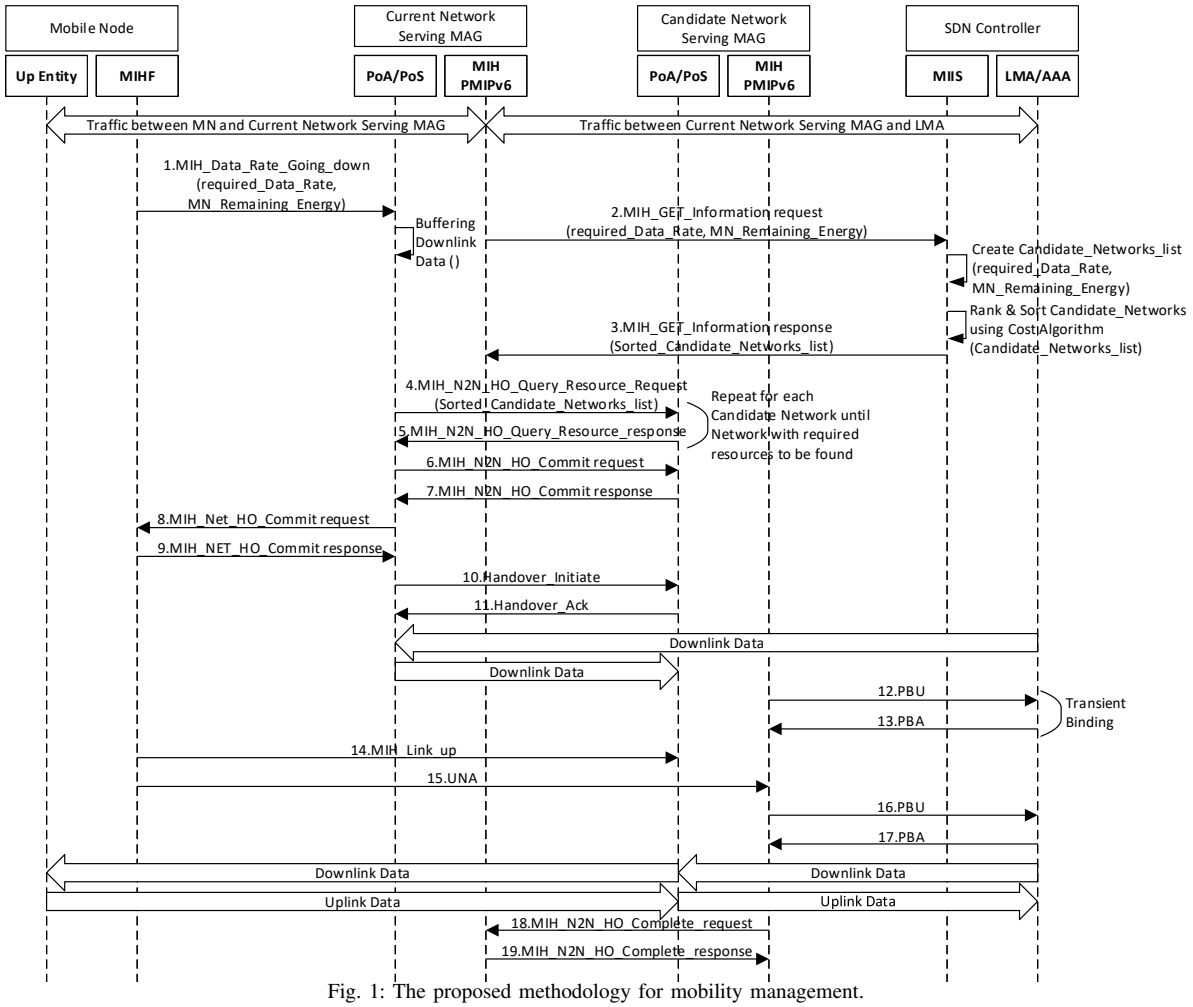

Fig. 1: The proposed methodology for mobility management.

therefore $C_{Threshold,Video} = 0.945$, $C_{Threshold,VoIP} = 0.661$ and $C_{Threshold,IoT} = 0.283$. When the observed $C_{j,s,i}$ drops below the specified threshold the MN should perform handover.

Indicatively, table II presents the network characteristic values that each j MN perceives for the s^{th} service from its current PoA i at the simulation time $t2$. The network characteristics include the $SINR_{j,i}$, the available bandwidth $B_{j,i}$ as well as the offered service quality $C_{j,s,i}$ for each service ($C_{j,Video,i}$, $C_{j,VoIP,i}$ and $C_{j,IoT,i}$). Accordingly, the MNs 0, 3, 5, 7 and 8 receive a service quality indicating that they should be connected to a new network.

TABLE II: The network characteristic values perceived from each MN from its current PoA at simulation time t2.

	MN0	MN1	MN2	MN3	MN4	MN5	MN6	MN7	MN8	MN9
SINRj,i (dB)	3.026	17.692	18.695	3.770	14.375	6.0526	15.333	6.052	6.969	16.428
Bj,I (MHz)	10	20	100	20	10	10	10	20	10	10
CVideo,j,i	-	2.322	12.921	0.538	0.981	-	1.043	-	0.484	1.113
CVoIP,j,i	0.288	1.625	9.045	0.377	0.687	-	0.730	1.819	0.339	0.779
CIoT,j,i	0.123	0.696	3.876	0.161	0.294	0.378	0.313	-	0.145	0.334
Csum,j,i	0.411	4.644	25.843	1.077	1.963	0.378	2.087	1.819	0.969	2.227
Handover required	Yes	No	No	Yes	No	Yes	No	Yes	Yes	No

Figure 3 presents the data rate perceived per MN during its movement across the access networks while either the proposed or the WFBH algorithms are applied for the VHO initiation and the network selection. At the aforementioned time $t2$ the proposed network selection algorithm decides that MN0 should perform a handover to the LTE-A Femtocell. MN3 should be connected to the LTE-A Pro FD-MIMO Macrocell, MN5 to the WAVE RSU 2, MN7 to the LTE-A Pro FD-MIMO Macrocell and MN8 to the LTE-A Femtocell. At the same time point, the WFBH network selection algorithm always selects the LTE-A Pro FD-MIMO Macrocell since it offers the highest rates. However, users with low battery levels (e.g. MN0, MN5 and MN8) would obtain data rates equal to zero after the simulation time $t3$, since the use of multiple antennas immediately consumes their remaining energy and cease operating. In the above cases, the proposed algorithm selects an alternative network and the user equipment remains functional for a longer time. The missing MNs from figure 3 (MN1, MN2, MN4, MN6 and MN9) remain to their current networks since they obtain satisfactory QoS.

B. Evaluation of VHO execution

The signaling cost of the proposed methodology is evaluated in comparison with the one obtained from the FMIPv6 [4] and the eFPMIPv6 [22] schemes.

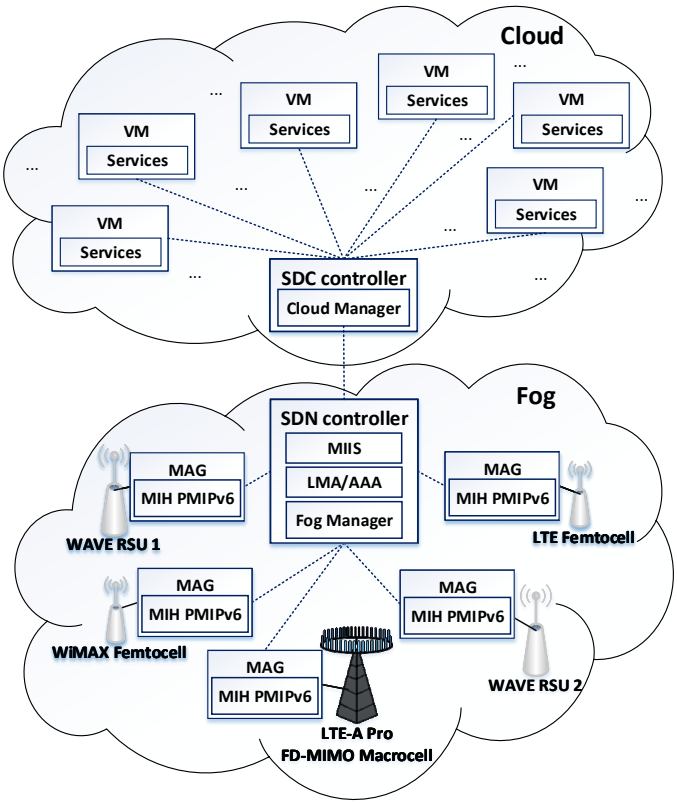

Fig. 2: The simulated topology.

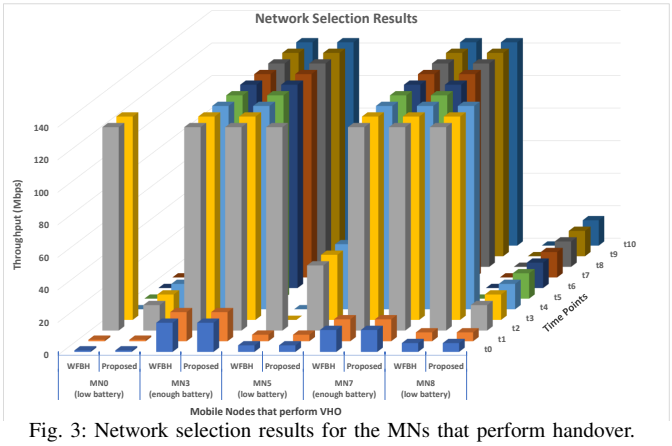

Fig. 3: Network selection results for the MNs that perform handover.

The signaling transmission cost is evaluated based on the number of hops that each message must perform (Table III) and the size of each message (Table IV) according to [6]. Consequently, the total signaling cost of the proposed scheme is calculated as follows:

TABLE III: The hops between the components of the considered topology.

Communicating Components	Number of Hops
$H_{MN,MAG}$	1
$H_{MAG,LMA}$	1
$H_{MAG,MIIS}$	1
$H_{MAG,MAG}$	2

$$Cost_{proposed} = \frac{P_f}{1-P_f} * H_{MN,MAG} * (M_1 + M_8 + M_9 + M_{14} + M_{15}) + 2 * H_{MAG,LMA} * (M_{12,16} + M_{13,17}) + H_{MAG,MIIS} * (M_2 + M_3) + H_{MAG,MAG} * (n * (M_4 + M_5) + M_6 + M_7 + M_{10} + M_{11} + M_{18} + M_{19})) \quad (2)$$

where P_f represents the connection failure probability and is supposed to be equal to 0.5 [6]. Also, n denotes the number of the available networks. Similarly, the signaling cost of FMIPv6 is calculated as follows:

$$Cost_{FMIPv6} = \frac{P_f}{1-P_f} * H_{MN,MAG} * (M_1 + M_4 + M_5 + M_8 + M_9 + M_{20} + M_{21}) + 3 * H_{MAG,LMA} * (M_{12,16} + M_{13,17}) + H_{MAG,MIIS} * (M_2 + M_3) + H_{MAG,MAG} * (n * (M_{5b} + M_{5c}) + M_6 + M_7 + M_{10} + M_{11} + M_{18} + M_{19}) \quad (3)$$

Finally, the signalling cost of the eFPMIPv6 is calculated as follows:

$$Cost_{eFPMIPv6} = \frac{P_f}{1-P_f} * H_{MN,MAG} * (M_1 + M_4 + M_5 + M_8 + M_9 + M_{14} + M_{15}) + 2 * H_{MAG,LMA} * (M_{12,16} + M_{13,17}) + H_{MAG,MIIS} * (M_2 + M_3) + H_{MAG,MAG} * (n * (M_{5b} + M_{5c}) + M_{6e} + M_{7e} + M_{18} + M_{19}) \quad (4)$$

TABLE IV: The cost of each message exchanged during the signaling process.

Message Name	Size (Bytes)	Abbreviation
MIH_Link_Going_down	78	M_1
MIH_GET_Information_request	1500	M_2
MIH_GET_Information_response	1500	M_3
MIH_Net_HO_Candidate_Query_request	63+11*n+8*m* n	M_4
MIH_Net_HO_Candidate_Query_response	77+101*m	M_5
MIH_N2N_HO_Query_Resource_request	150+11*m	M_{5b}
MIH_N2N_HO_Query_Resource_response	165	M_{5c}
MIH_N2N_HO_Commit_request	213	M_6
MIH_N2N_HO_Commit_request (Extended)	264	M_{6e}
MIH_N2N_HO_Commit_response	92	M_7
MIH_N2N_HO_Commit_response (Extended)	92	M_{7e}
MIH_Net_HO_Commit_request	122	M_8
MIH_Net_HO_Commit_response	103	M_9
Handover_Initiate	72	M_{10}
Handover_Ack	32	M_{11}
PBU	76	$M_{12,16}$
PBA	52	$M_{13,17}$
MIH_Link_up	95	M_{14}
UNA	52	M_{15}
MIH_N2N_HO_Complete_request	109	M_{18}
MIH_N2N_HO_Complete_response	112	M_{19}
RS	16	M_{20}
RA	64	M_{21}

Figure 4 compares the signaling costs obtained from each scheme in the simulated network topology. As it can be observed, the signaling cost of the proposed scheme is lower than the one observed in the case of FMIPv6 and eFPMIPv6, due to the additional messages that these schemes exchange during the VHO execution.

Furthermore, figure 5 presents the signaling costs obtained from the aforementioned schemes, as the number of hops between the previous and the next MAGs ($H_{MAG,MAG}$) increases. As it can be observed, as the $H_{MAG,MAG}$ increases

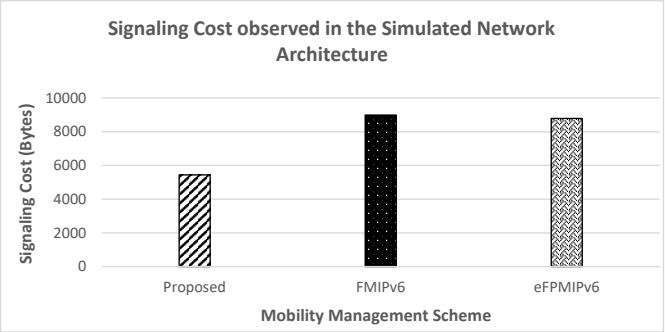

Fig. 4: The signaling cost of the proposed scheme in comparison with the FMIPv6 and eFPMIPv6 schemes.

the signaling cost also increases. However, in all cases the signaling cost of the proposed scheme is lower than the one observed from the other two schemes.

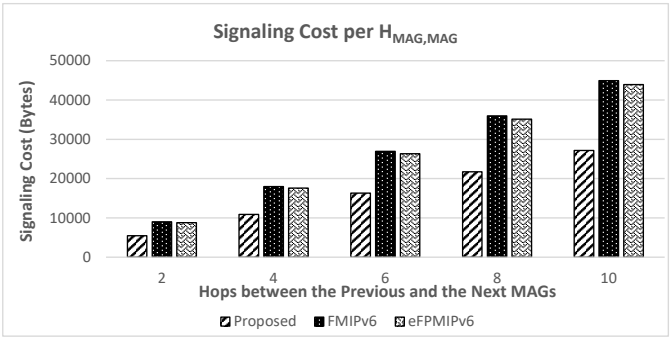

Fig. 5: The signaling cost of each scheme considering the hops between the Previous and the Next Mags.

V. Conclusion

This paper proposes an energy aware mobility management scheme for supporting modern services in 5G network architectures. The discussed scheme implements both the VHO initiation, the Network Selection and the VHO execution. The described methodology is evaluated through simulations in a heterogeneous wireless network architecture consisting of LTE-A, 802.16 WiMAX and 802.11p WAVE networks. Performance evaluation showed that the proposed scheme outperforms existing methods by ensuring the Always Best Connected (ABC) principle, while at the same time it increases the time that the MN remains functional. Furthermore, the proposed MIH-enhanced FPMIPv6 scheme results to decreased signaling cost during VHO in comparison with relative mobility management approaches.

ACKNOWLEDGEMENTS

This work is partly supported by the University of Western Macedonia Research Committee.

References

[1] T. Han, S. Li, Y. Zhong, Z. Bai, and K.-S. Kwak, "5g software-defined heterogeneous networks with cooperation and partial connectivity," *IEEE Access*, vol. 7, pp. 72 577–72 590, 2019.

[2] H. Anandakumar, K. Umamaheswari, and R. Arulmurugan, "A study on mobile ipv6 handover in cognitive radio networks," in *International Conference on Computer Networks and Communication Technologies*. Springer, 2019, pp. 399–408.

[3] M. K. Rana, B. Sardar, S. Mandal, and D. Saha, "Implementation and performance evaluation of a mobile ipv6 (mipv6) simulation model for ns-3," *Simulation Modelling Practice and Theory*, vol. 72, pp. 1–22, 2017.

[4] G. Su, P. You, and S. Yong, "Comparative handover performance analysis of mipv6 and fmipv6 in leo satellite networks," in *2017 International Conference on Network and Information Systems for Computers (ICNISC)*. IEEE, 2017, pp. 30–36.

[5] S. M. Raza, D. S. Kim, D. Shin, and H. Choo, "Leveraging proxy mobile ipv6 with sdn," *Journal of Communications and Networks*, vol. 18, no. 3, pp. 460–475, 2016.

[6] V. Sharma, J. Guan, J. Kim, S. Kwon, I. You, F. Palmieri, and M. Collotta, "Mih-spfp: Mih-based secure cross-layer handover protocol for fast proxy mobile ipv6-iot networks," *Journal of Network and Computer Applications*, vol. 125, pp. 67–81, 2019.

[7] A. Michalas, A. Sgora, and D. D. Vergados, "An integrated mih-fpmipv6 mobility management approach for evolved-packet system architectures," *Journal of Network and Computer Applications*, vol. 91, pp. 104–119, 2017.

[8] "TS 24.302 (V14.3.0): Access to the 3GPP Evolved Packet Core (EPC) via non-3GPP access networks (Rel.14)," *Technical Specification, 3GPP*, 2017.

[9] X. Yan, Y. A. Şekercioğlu, and S. Narayanan, "A survey of vertical handover decision algorithms in fourth generation heterogeneous wireless networks," *Computer networks*, vol. 54, no. 11, pp. 1848–1863, 2010.

[10] M. Lahby, L. Cherkaoui, and A. Adib, "New multi access selection method based on mahalanobis distance," *Applied Mathematical Sciences*, vol. 6, no. 53-56, pp. 2745–2760, 2012.

[11] I. Martinez and V. Ramos, "Netanpi: A network selection mechanism for lte traffic offloading based on the analytic network process," in *2015 36th IEEE Sarnoff Symposium*. IEEE, 2015, pp. 117–122.

[12] S. Kaur, S. K. Sehra, and S. S. Sehra, "A framework for software quality model selection using topsis," in *2016 IEEE International Conference on Recent Trends in Electronics, Information & Communication Technology (RTEICT)*. IEEE, 2016, pp. 736–739.

[13] E. Skondras, A. Sgora, A. Michalas, and D. D. Vergados, "An analytic network process and trapezoidal interval-valued fuzzy technique for order preference by similarity to ideal solution network access selection method," *International Journal of Communication Systems*, vol. 29, no. 2, pp. 307–329, 2016.

[14] I. Bisio, C. Braccini, S. Delucchi, F. Lavagetto, and M. Marchese, "Dynamic multi-attribute network selection algorithm for vertical handover procedures over mobile ad hoc networks," in *2014 IEEE international conference on communications (ICC)*. IEEE, 2014, pp. 342–347.

[15] I. Lassoued, J.-M. Bonnin, Z. B. Hamouda, and A. Belghith, "A methodology for evaluating vertical handoff decision mechanisms," in *Seventh International Conference on Networking (ICN 2008)*. IEEE, 2008, pp. 377–384.

[16] E. Roszkowska and D. Kacprzak, "The fuzzy saw and fuzzy topsis procedures based on ordered fuzzy numbers," *Information Sciences*, vol. 369, pp. 564–584, 2016.

[17] M. Drissi, M. Oumsis, and D. Aboutajdine, "A fuzzy ahp approach to network selection improvement in heterogeneous wireless networks," in *International Conference on Networked Systems*. Springer, 2016, pp. 169–182.

[18] "Network simulator 3 (ns3)," https://www.nsnam.org/, accessed: 2020.

[19] "TS 123.501 (V15.2.0): System Architecture for the 5G System (Rel.15)," *Technical Specification, 3GPP*, 2018.

[20] "TS 123.203 (V12.6.0): LTE Policy and charging control architecture (Rel.12)," *Technical Specification, 3GPP*, 2014.

[21] Y. Wang, R. Djapic, A. Bergström, I. Z. Kovács, D. Laselva, K. Spaey, and B. Sas, "Performance of wlan rss-based son for lte/wlan access network selection," in *2014 11th International Symposium on Wireless Communications Systems (ISWCS)*. IEEE, 2014, pp. 460–464.

[22] L. Zhang and Y.-C. Tian, "An enhanced fast handover triggering mechanism for fast proxy mobile ipv6," *Wireless Networks*, vol. 24, no. 2, pp. 513–522, 2018.